

Electromagnetic Force on Anisotropic-Conducting Film

Dan Xia*

Abstract—Electromechanical interaction between slow electromagnetic wave and anisotropic-conducting film is investigated. The physical effects associated with anisotropic-conducting film are revealed by electromagnetic theory and validated by experiment, and they have established the working principles for a class of electromechanical sensors and/or actuators, which have continuously moving part, and are sensitive to the amplitude and the direction of electromagnetic forces or fields and well able to reflect the resonance characteristics. The revealed and validated physical effects may have significance in quite different science and engineering fields and in wide frequency bands from RF to optics.

1. INTRODUCTION

The progress in microelectromechanical systems (MEMS) requires wireless (RF and microwave) systems for lower weight, volume, power consumption and cost with increased functionality, frequency of operation and component integration, and it is driving the development of new RF or microwave MEMS components and system architectures. The reported device types include switches, impedance tuners, tunable or reconfigurable filters, phase shifters and MEMS-based antennas [1–8]. However, it is hard to find a report on wireless devices playing a similar role of motor or actuator with continuously moving parts, because the principles based on rotating electric or magnetic field and independent electric and magnetic circuits will never work in RF or microwave frequency.

Different from microelectronics, MEMS usually have a concern with electromechanical kinetic and dynamic principles in components or devices. The requirement on converting RF/microwave energy to motion or kinetic energy arose as early as 1960s. So called parametric motor or microwave motor [9, 10] appeared at that period. That motor was essentially a DC motor with a rectifying antenna, inserted inside the waveguide to pick up and rectify the microwave energy into DC energy then feed it to the motor coil [11]. More recently, extensive research on micromachined microwave actuator [12] has been done to meet a number of unique applications, such as sliding transmission-line tuners for dynamic tuning of MMIC circuits after fabrication. The most promising driving and controlling candidate seems to be electrostatic actuator, but there are still some major problems. For example, rather high operating voltage and inherent non-linearity [13, 14] remain to be solved for this kind of actuator. Moreover, even if the above mentioned actuators can satisfy certain requirements for particular application, they cannot fulfill the direct conversion of RF or microwave energy into kinetic energy.

In physics, the scientists have found that electromagnetic (EM) force, referred to radiation pressure in optical frequency band, can manipulate micro-objects [15] and even make micro-objects rotating [16]. The effort has continued so far to enhance radiation pressure [17], but generally it is probably still not big enough for most MEMS applications. As a part of this effort, our research is concentrated on special physical effects arising from electromechanical interaction between slow EM wave and anisotropic-conducting film (ACF). Here we report the analysis and experimental validation of this interaction to establish the working principles for a novel ACF transducer.

Received 2 April 2016, Accepted 8 June 2016, Scheduled 23 June 2016

* Corresponding author: Dan Xia (xiadan@tjut.edu.cn).

The author is with the Tianjin Key Laboratory of Film Electronic and Communication Device, School of Electronic Information Engineering, Tianjin University of Technology, Tianjin 300384, China.

2. ELECTROMECHANICAL INTERACTION ON ACF

To analyze the electromechanical interaction, we consider a simplified planar ACF model excited by EM wave as shown in Fig. 1. ACF is at $z = 0$ and moving at the velocity $\vec{v} = \vec{x}_0 v$, and its anisotropic surface conductivity represented in moving frame is

$$\vec{\sigma}' = \vec{y}_0 \vec{y}_0 \sigma \quad (1)$$

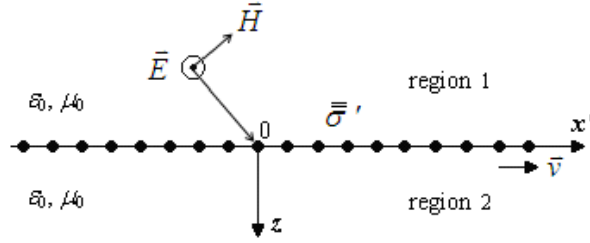


Figure 1. Structure diagram of ACF under the incidence of TE wave.

Both regions 1 and 2 are stationary free space with permittivity ε_0 and permeability μ_0 . The exciting TE (y -polarized) electrical field of EM wave has the form as

$$\vec{E} = \vec{y}_0 E e^{-jk_z z} e^{j(\omega t - \alpha x)} \quad (2)$$

in which E is the wave amplitude, ω the angular frequency, and α the propagation constant in x -direction. For a slow wave, α is greater than propagation constant $k_0 = \omega/c$, where $c = 1/\sqrt{\mu_0 \varepsilon_0} = 3 \times 10^8$ m/s is the light speed in free space, and therefore the phase velocity in x -direction

$$v_p = \omega/\alpha \quad (3)$$

is less than the light speed $c = \omega/k_0$ in free space [18]. Considering reflection and transmission, the total fields in regions i ($i = 1, 2$) can be expressed as

$$\vec{E}_i = \vec{y}_0 V_i(z) e^{j(\omega t - \alpha x)} \quad (4)$$

with mode voltages

$$V_1(z) = E e^{-jk_z z} + R e^{jk_z z} \quad (5)$$

$$V_2(z) = T e^{-jk_z z} \quad (6)$$

R and T are the amplitudes of reflected and transmitted waves to be determined, corresponding to the E -field amplitude of incident wave E . The propagation constant in z -direction is

$$k_z = \sqrt{\omega^2/c^2 - \alpha^2} = -j\gamma \quad (7)$$

and

$$\gamma = \sqrt{\alpha^2 - \omega^2/c^2} = \omega \sqrt{1/v_p^2 - 1/c^2} \quad (8)$$

is real for slow wave.

By using of Maxwell's equation $\nabla \times \vec{E} = -\mu_0 \frac{\partial \vec{H}}{\partial t}$, H -fields can be derived as

$$\vec{H}_i = \left[-\vec{x}_0 I_i(z) + \vec{z}_0 \frac{\alpha}{\omega \mu_0} V_i(z) \right] e^{j(\omega t - \alpha x)} \quad (9)$$

with mode currents

$$I_1(z) = Y \left[E e^{-jk_z z} - R e^{jk_z z} \right] \quad (10)$$

$$I_2(z) = Y T e^{-jk_z z} \quad (11)$$

and

$$Y = \frac{k_z}{\omega\mu_0} = -j\frac{\gamma}{\omega\mu_0} = -j\frac{\sqrt{1/v_p^2 - 1/c^2}}{\mu_0} \quad (12)$$

is characteristic admittance.

To count the contribution of ACF, it is necessary to express the fields in moving frame. For a speed v much smaller than the light speed c , Galilean transformations $x' = x - vt$, $y' = y$, $z' = z$ and $t' = t$ can be applied [19]. The fields in moving frame are

$$\vec{E}'_i = \vec{E}_i + v \times \mu_0 \vec{H}_i = \vec{y}_0 \left(1 - \frac{v}{v_p}\right) V_i(z) e^{j(\omega t - \alpha x)} \quad (13)$$

$$\vec{H}'_i = \vec{H}_i - v \times \varepsilon_0 \vec{E}_i = \left[-\vec{x}_0 I_i(z) + \vec{z}_0 \left(\frac{\alpha}{\omega\mu_0} - \varepsilon_0 v\right) V_i(z)\right] e^{j(\omega t - \alpha x)} \quad (14)$$

The boundary conditions at the interfaces $z = 0$ are

$$\begin{cases} \vec{z}_0 \times \left(\vec{E}'_2 - \vec{E}'_1\right) \Big|_{z=0} = 0 \\ \vec{z}_0 \times \left(\vec{H}'_2 - \vec{H}'_1\right) \Big|_{z=0} = \vec{J} \end{cases} \quad (15)$$

where

$$\vec{J} = \vec{\sigma}' \cdot \left(\vec{E}'_1 + \vec{E}'_2\right) \Big|_{z=0} \quad (16)$$

is the equivalent current density induced in ACF. Both tangential (parallel to v) component of H -field and current density are invariant for Galilean transformation, hence the boundary conditions are the same as those in stationary frame. Substituting the fields in moving frame into Eqs. (15) and (16) can obtain

$$\begin{cases} T - (E + R) = 0 \\ YT - Y(E - R) = -2\sigma \left(1 - \frac{v}{v_p}\right) T \end{cases} \quad (17)$$

Most concerned transmission coefficient τ can be solved as follows

$$\tau = \frac{T}{E} = \frac{Y}{Y + \sigma \left(1 - \frac{v}{v_p}\right)}. \quad (18)$$

3. FORCE-SPEED DEPENDENCE

Nothing but the Lorentz force makes ACF to move. The force density can be derived by using

$$\vec{F} = \vec{J} \times \vec{B}'_2 = \vec{J} \times \mu_0 \vec{H}'_2 \quad (19)$$

Suppose that mechanically the film is only possible to move in x -direction so that we only pay attention to the x -component of EM force density F_x . It is related to the z -component of flux density at $z = 0$

$$B'_{2z} = \left(\frac{1}{v_p} - \frac{v}{c^2}\right) T e^{j(\omega t - \alpha x)} \quad (20)$$

and the y -component of the current density

$$J = 2\sigma \left(1 - \frac{v}{v_p}\right) T e^{j(\omega t - \alpha x)} \quad (21)$$

To keep the film moving continuously in x -direction, it is required that the effective (average) force density in x -direction $\langle F_x \rangle$ is nonzero. $\langle F_x \rangle$ can be obtained by integrating the EM force density over space period $2\pi/\alpha$ and time period $2\pi/\omega$, respectively, and the result is

$$\langle F_x \rangle = \text{Re} \left(\frac{JB'_{2z}}{2} \right) \quad (22)$$

where * denotes complex conjugate. Substituting Eqs. (20) and (21) into Eq. (22), it follows that

$$\langle F_x \rangle = \sigma \left(1 - \frac{v}{v_p}\right) \left(\frac{1}{v_p} - \frac{v}{c^2}\right) TT^* \quad (23)$$

Then from (18) and (12),

$$\langle F_x \rangle = \frac{\sigma \left(1 - \frac{v}{v_p}\right) \left(\frac{1}{v_p} - \frac{v}{c^2}\right)}{1 + \frac{\sigma^2 \left(1 - \frac{v}{v_p}\right)^2 \mu_0^2}{1/v_p^2 - 1/c^2}} E^2 \quad (24)$$

From Eq. (24) it is obvious that $\langle F_x \rangle$ depends on wave parameters E and v_p (the ratio ω/α instead of ω or α itself), and film parameters σ and v . The EM force is proportional to a factor $(1/v_p - v/c^2)$, or roughly speaking, proportional to $1/v_p$ since $v \ll c$, which means that “slower” wave can cause more significant EM force. It is a condition rather easy to realize. Once wave parameters are given, say $E = 1 \text{ V/m}$ and $v_p = 0.01c$, we can draw force-speed curves for different surface conductivities σ as shown in Fig. 2. The main features of ACF transducer can be abstracted from the curves: at synchronous speed $v = v_p$, the force is always equal to zero, and at point $v = 0$, the starting force $\langle F_x \rangle_s$ is generally non-zero; at certain speed near but different from synchronous speed v_p , the force can get the maximum value; less conductivity σ leads to larger starting force and bigger speed slip ($v_p - v$) for the maximum force. Besides, the force can be positive or negative for speed v less or greater than synchronous speed v_p , respectively, corresponding to the conversion of EM to mechanic energy or vice versa, just as in the interaction between EM wave and moving charged particles.

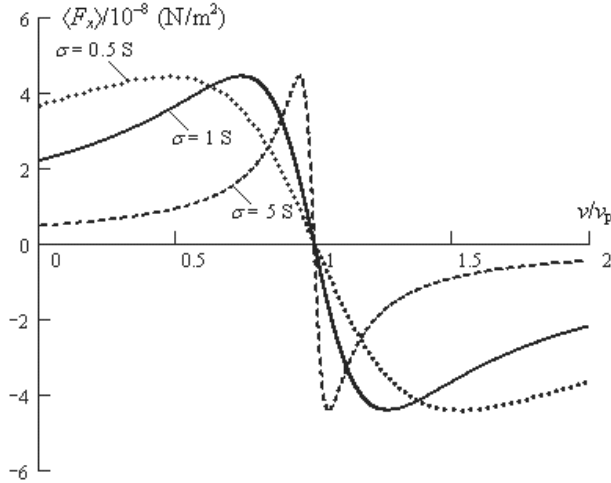


Figure 2. Force-speed curves for different surface conductivity.

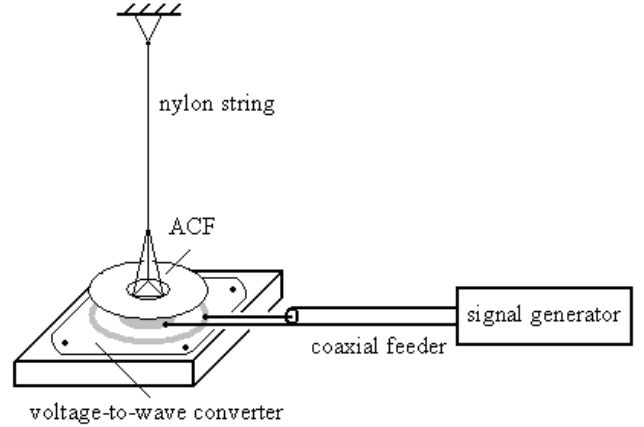


Figure 3. Schematic diagram of experimental device.

4. EXPERIMENTAL VALIDATION

As shown in Fig. 3, an experiment is used to observe the motion of ACF under the EM force and to show how the force density transduces the wave parameters. The film is on a disk-shaped substrate and with a circular array of etched slots to form an ACF (in Fig. 4(a)) with the anisotropic conductivity defined by Eq. (1). For the convenience and accuracy of measurement, ACF with the substrate hung by a nylon string is assembled as a torsion pendulum [20] so that it can rotate as the EM force is exerted and finally reach the balanced angle θ as the EM torque equals the torque of the nylon string. The EM torque is proportional to $\langle F_x \rangle|_{v=0}$, and it is nothing but the starting force $\langle F_x \rangle_s$. From Eq. (24) it is

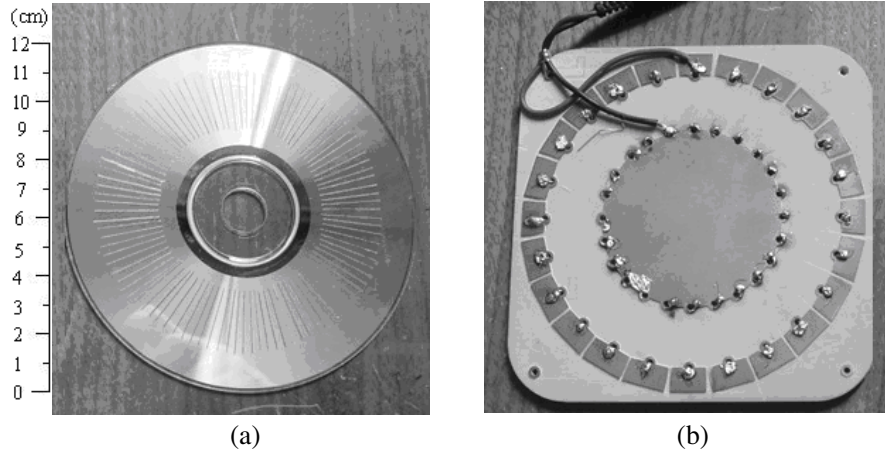


Figure 4. Physical maps of ACF and voltage-to-wave converter used in the experiment.

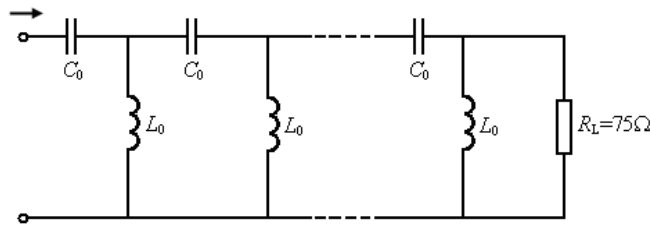


Figure 5. Layout of transmission line used in the experiment.

Table 1. Balanced angles θ at different frequencies.

f (MHz)	150	266	290	340	440	540	650	750	850	1000
θ (degree)	-15	-11.3	15	33.3	37.5	37.5	37.5	37.5	56.3	41.3

obtained that

$$\langle F_x \rangle_s = \frac{\frac{\sigma}{v_p}}{1 + \frac{\sigma^2 \mu_0^2}{1/v_p^2 - 1/c^2}} E^2 \tag{25}$$

On the other hand, by using balanced angle θ this force of the nylon string can be expressed as

$$\langle F_x \rangle_s = K\theta \tag{26}$$

where K is a constant depending on the springiness and radius of the torsion pendulum.

The external EM field is excited by a stationary high-pass or left-handed transmission line of which the appearance is similar to the shape of ACF. The transmission line plays the role of a voltage-to-wave converter (in Fig. 4(b)) and is located as close to the bottom of ACF as possible. When the transmission line as shown in Fig. 5 is terminated with a matched g load of $75\ \Omega$ at one port and excited by a high frequency voltage from a signal generator at another port, there is travelling wave as defined by Eq. (2) on the surfaces of ACF.

In the experiment, EM force density $\langle F_x \rangle$ exerted on ACF and makes it moving. Its movement can be observed in full frequency range from 150 MHz to 1000 MHz of the signal generator with the output voltage 27 V in all the tests. The measured balanced angles θ of the torsion pendulum at different frequencies f are listed in Table 1.

The measured data reveal that EM force density can change the direction in different frequency ranges. So far, no formulation on ACF has given support to such an experiment phenomenon. Therefore,

we have to turn to the wave behavior instead of ACF itself. Considering the effect of stray fields, the converter has to be more exactly modeled as a composite right/left-handed transmission line [21] instead of a pure left-handed transmission line. Under the condition of balanced resonances, the phase velocity of travelling wave can be expressed [22] as

$$v_p = \frac{\omega^2 \omega'_R}{\omega^2 - \omega_0^2} \quad (27)$$

where ω_0 is the resonance frequency,

$$\omega'_R = \frac{1}{\sqrt{L'_R C'_R}} \quad (28)$$

ω'_R is of the same dimensionality as v_p (m/s) in Eq. (3), in which L'_R (H/m) and C'_R (F/m) are stray inductance and capacitance per unit length, respectively.

A typical phase velocity-to-frequency curve from Eq. (27) is shown in Fig. 6. One can figure out from the curve that the phase velocity, and starting force in turn, can change the direction in different frequency bands in the experiment. Substituting Eq. (27) into Eq. (25) and taking $\omega_0 = 2\pi \times 280 \times 10^6$ rad/s, $\omega'_R = 0.00006c$ and $\sigma = 1$ S, the values of $\langle F_x \rangle_s$ are calculated and shown in Fig. 7. Taking $K = 1 \times 10^{-6}$ N/(m²·degree), the measured balanced angles θ can transform into the values of $\langle F_x \rangle_s$ from Eq. (26), which are also shown in Fig. 7 for comparison. Although the calculated results are not so ideally agree with the measured ones, the theory can still give a convinced explanation of the complex behavior of EM wave in a composite right/left-handed transmission line [23]. In other words, the ACF sensor is sensitive to the amplitude, in addition to the direction of EM force or field. The amplitude also depends on the phase velocity of EM wave, and the resonance characteristics can also be well reflected. Those are valuable properties of an electromechanical transducer.

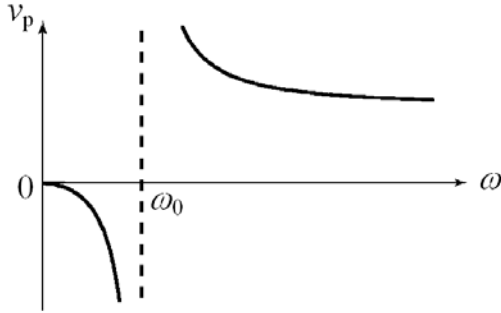


Figure 6. Phase velocity-to-frequency curve of composite right/left-handed transmission line.

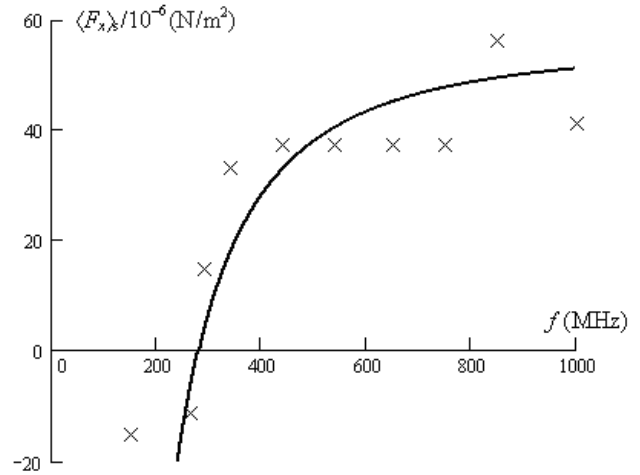


Figure 7. Comparison of measured (\times) and calculated (solid line) forces.

5. CONCLUSION

Based on EM theory, the EM force exerted on ACF is investigated. The force-speed dependence is the function of wave parameters (amplitude E and phase velocity v_p) and film parameters (surface conductivity σ and moving velocity v), implying that ACF can play the role of a transducer from one above mentioned wave or film parameter to another. The physical effects associated with ACF revealed by EM theory and validated by the experiment here have established the working principles for a class of novel sensors and/or actuators with continuously moving part, and may have significance in other quite different science and engineering fields and in wide frequency bands covering RF, microwave and optics [16].

REFERENCES

1. Santos, H. J. D. L. and R. J. Richards, "MEMS for RF microwave wireless applications: The next wave — Part II," *Microwave J.*, Vol. 44, No. 7, 41–47, 2001.
2. Lucyszyn, S., "Review of radio frequency microelectromechanical systems technology," *IEE Proc. Sci. Meas. Technol.*, Vol. 151, No. 2, 93–103, 2004.
3. Pothier, A., J. C. Orlianges, G. Z. Zheng, C. Champeaux, A. Catherinot, D. Cros, P. Blondy, and J. Papapolymerou, "Low-loss 2-bit tunable bandpass filters using MEMS DC contact switches," *IEEE Trans. Microw. Theory Techn.*, Vol. 53, No. 1, 354–360, 2005.
4. Liu, C., "Recent developments in polymer MEMS," *Adv. Mater.*, Vol. 19, No. 22, 3783–3790, 2007.
5. Entesari, K., K. Obeidat, A. R. Brown, and G. M. Rebeiz, "A 25–75-MHz RF MEMS tunable filter," *IEEE Trans. Microw. Theory Techn.*, Vol. 55, No. 11, 2399–2405, 2007.
6. Lopez, J. L., J. Verd, A. Uranga, J. Giner, G. Murillo, F. Torres, G. Abadal, and N. Barniol, "A CMOS-MEMS RF-tunable bandpass filter based on two high-22-MHz polysilicon clamped-clamped beam resonators," *IEEE Electr. Device Lett.*, Vol. 30, No. 7, 718–720, 2009.
7. Jaafar, H., F. L. Nan, and N. A. M. Yunus, "Design and simulation of high performance RF MEMS series switch," *IEEE Regional Symposium on Micro and Nanoelectronics (RSM)*, 349–353, Kota Kinabalu, Malaysia, September 2011.
8. Stamper, A. K., C. V. Jahnes, S. R. Dupuis, A. Gupta, Z. X. He, R. T. Herrin, S. E. Luce, J. Maling, D. R. Miga, W. J. Murphy, E. J. White, S. J. Cunningham, D. R. De Reus, I. Vitomirov, and A. S. Morris, "Planar MEMS RF capacitor integration," *16th International Solid-State Sensors, Actuators and Microsystems Conference (Transducers)*, 1803–1806, Beijing, China, June 2011.
9. Stockman, H. E., "Parametric oscillatory and rotary motion," *Proc. Inst. Radio Engrs. (Correspondence)*, Vol. 48, 1157–1158, 1960.
10. Garnier, R. C. and K. Ishii, "Microwave motor," *Proc. Inst. Radio Engrs. (Correspondence)*, Vol. 52, 1380–1381, 1964.
11. Steinhoff, R. W. and T. K. Ishii, "Pickup antenna for waveguide motors," *IEEE Trans. Microw. Theory Techn. (Correspondence)*, Vol. 14, No. 9, 438, 1966.
12. Larson, L. E., R. H. Hackett, M. A. Melendes, and R. F. Lohr, "Micromachined microwave actuator (MIMAC) technology—a new tuning approach for microwave integrated circuits," *IEEE Microwave & Millimeter-wave Monolithic Circuits Symposium*, 27–30, Boston, MA, USA, June 1991.
13. Krylov, S., I. Harari, and Y. Cohen, "Stabilization of electrostatically actuated microstructures using parametric excitation," *J. Micromech. Microeng.*, Vol. 15, No. 6, 1188–1204, 2005.
14. Zhao, X., C. K. Reddy, and A. H. Nayfeh, "Nonlinear dynamics of an electrically driven impact microactuator," *Nonlinear Dynamics*, Vol. 40, No. 3, 227–239, 2005.
15. Ashkin, A., "History of optical trapping and manipulation of small-neutral particle, atom, and molecules," *IEEE J. Sel. Top. Quantum Electron.*, Vol. 6, No. 6, 841–856, 2000.
16. Higurashi, E., O. Ohguchi, T. Tamamura, H. Ukita, and R. Sawada, "Optically induced rotation of dissymmetrically shaped fluorinated polyimide micro-objects in optical traps," *J. Appl. Phys.*, Vol. 82, No. 6, 2773–2779, 1997.
17. Mizrahi, A., M. Horowitz, and L. Schächter, "Torque and longitudinal force exerted by eigenmodes on circular waveguides," *Phys. Rev. A*, Vol. 78, No. 2, 0238021–6, 2008.
18. Xia, D. and T. L. Dong, "Reflection and transmission of electromagnetic slow-waves by a uniformly moving dielectric slab," *Chinese Sci. Bull.*, Vol. 55, No. 34, 3875–3879, 2010.
19. Kong, J. A., *Electromagnetic Wave Theory*, EMW Publishing, Cambridge, MA, USA, 2005.
20. Braginsky, V. B. and A. B. Manukin, *Measurement of Weak Forces in Physics Experiments*, University of Chicago Press, Pasadena, Chicago, CA, USA, 1977.
21. Günel, T., "A genetic approach to the synthesis of composite right/left-handed transmission line impedance matching sections," *Int. J. Electron. Commun. (AEÜ)*, Vol. 61, No. 7, 459–462, 2007.
22. Caloz, C. and T. Itoh, *Electromagnetic Metamaterials: Transmission Line Theory and Microwave Applications: The Engineering Approach*, John Wiley & Sons, Inc., Hoboken, New Jersey, USA,

2006.

23. Xia, D., R. X. Yao, P. Li, G. Feng, and T. L. Dong, "Measurement of transition frequency of composite transmission line model," *Asia-Pacific Power & Energy Engineering Conference (APPEEC)*, 1-2, Wuhan, China, March 2011.